Effective Decomposition of Water Vapor in Radio-Frequency Plasma with Carbon Deposition on Vessel Wall*)

Makoto OYA, Ryosuke IKEDA[1)] and Kazunari KATAYAMA

Faculty of Engineering Sciences, Kyushu University, Fukuoka 816-8580, Japan

[1)]*Interdisciplinary Graduate School of Engineering Sciences, Kyushu University, Fukuoka 816-8580, Japan*

(Received 12 January 2022 / Accepted 20 April 2022)

In a thermonuclear fusion reactor, a fuel cycle system that recovers and reuses unburnt hydrogen isotopes is indispensable. Oxygen (O) and carbon (C) impurities are chemically combined with the unburnt hydrogen isotopes and exhausted from the plasma vessel of the fusion reactor. The impurities must be decomposed in the fuel cycle system to recover the hydrogen isotopes, especially tritium. In this study, a flow-type reactor using a radio-frequency (RF) plasma was applied to decompose water vapor (H_2O) molecules. The effect of C deposition on the vessel wall (stainless steel) was confirmed experimentally to promote reactions relating to the decomposition. At RF powers of 30 - 150 W, the decomposition ratio was around 30% with an argon gas mixed with 5% H_2O at the pressure of 100 Pa (5 Pa for H_2O) and the flow rate of 20 sccm (1 sccm for H_2O). The decomposition was enhanced by C depositions on the vessel wall; the decomposition ratio was largely increased to be 75% at the RF power of 150 W. Reasons for the increased ratio may be a reduction of O atoms and molecules and a production of carbon monoxide through the interaction with C depositions. The reduction of O products promoted the decomposition of H_2O in the plasma because the recombination of O and H can be suppressed.

Keywords: fusion reactor, fuel cycle, tokamak exhaust process system, hydrogen isotope recovery, water vapor, plasma decomposition, carbon deposition

DOI: 10.1585/pfr.17.2405087

1. Introduction

Unburnt fuels, i.e., deuterium (D) and tritium (T), will be exhausted from a vacuum vessel in a thermonuclear fusion reactor. To recycle the fuels back to the reactor, a recovery system of hydrogen isotopes from the exhaust gas is indispensable for an efficient fuel cycle [1]. The exhaust gases contain chemical compounds, such as water vapor (H_2O) and hydrocarbons (e.g., CH_4), deuterated and tritiated. Therefore, the hydrogen isotopes are required to be recovered by decomposition of the chemical compounds. For the tokamak exhaust process (TEP) system in ITER [2, 3], chemical reactors, such as catalytic reactor (coupled by palladium membrane reactor) [4] and ceramic electrolysis cell [5], are considered to decompose the chemical compounds. However, the heating and pressurization, even atmospheric pressure, should be avoided to prevent hydrogen isotopes from permeating out of the reactor. Different catalysts are used for each chemical compound. Furthermore, the catalysts can be degraded due to carbon (C) dust produced by hydrocarbon decomposition during long-term decomposition.

Previous studies conducted H_2O decomposition using radio-frequency (RF) plasma for energy applications [6]. In the 1980s [7], a 13.56-MHz RF plasma was used to synthesize hydrogen peroxide (H_2O_2). Approximately 60% of H_2O gas was decomposed at a low flow rate (0.26 - 1.0 sccm), low pressure (~40 Pa), and low RF power (20 and 50 W). Additionally, a much higher RF power range was explored from 250 to 1,000 W [8].

In our previous study, we investigated a flow-type reactor using an RF plasma to recover hydrogen isotopes from hydrocarbons [9–12]. In the reactor, decomposition of the hydrocarbons occurred through collision sequences with energetic electrons and ions in the plasma [12]. In a previous experiment [9], a helium plasma decomposed almost all (> 99%) methane (CH_4) molecules at low RF power (< 10 W) and low pressure (250 Pa). However, C was produced by the decomposition and deposited on a vessel wall. The C deposition retained a part of hydrogen (H) products, which reduced H recovery efficiency.

In this study, our plasma reactor was applied to decomposition of H_2O. Furthermore, in order to explore the possibility to improve the decomposition ratio, the effect of C deposition on the vessel wall was investigated experimentally with respect to plasma-wall interactions.

2. Experiments

2.1 Experimental setup and procedure

Figure 1 shows a schematic of our experimental setup, including a flow-type plasma reactor. The plasma reactor was a cylindrical vessel made of stainless steel with

author's e-mail: moya@aees.kyushu-u.ac.jp

*) This article is based on the presentation at the 30th International Toki Conference on Plasma and Fusion Research (ITC30).

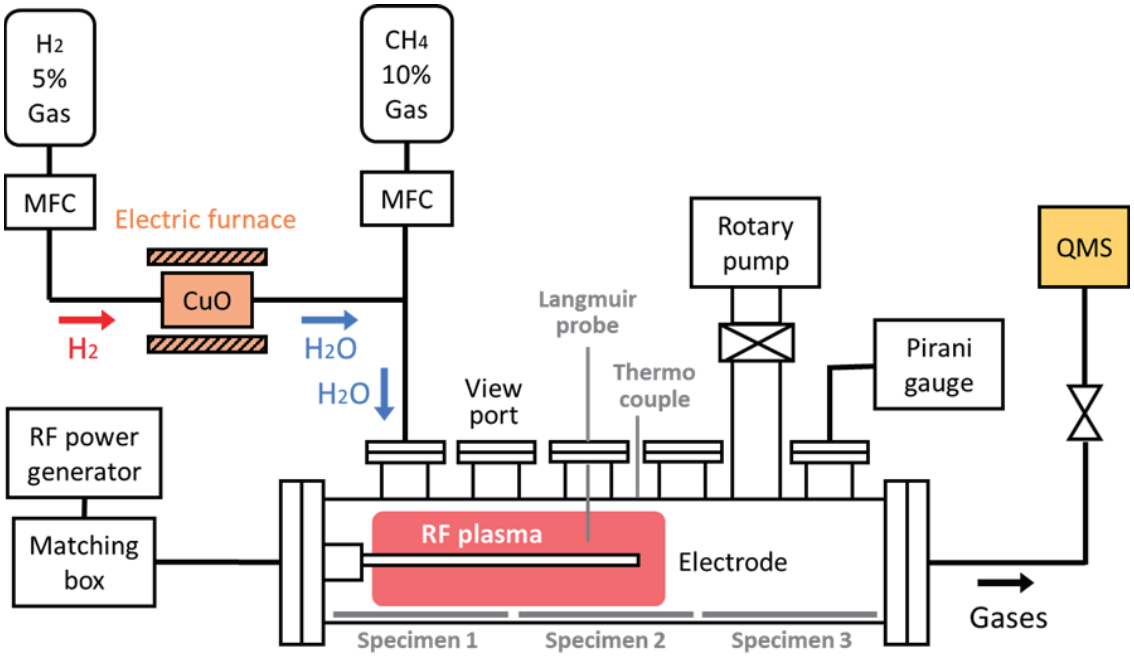

Fig. 1 Schematic of the experimental setup of a flow-type plasma reactor. In the reactor, three long and narrow specimens to analyze chemical composition of the surface were placed on a vessel wall.

an inner diameter of 35 mm. An RF power at 13.56 MHz was supplied to a rod with a diameter and length of 8 and 260 mm, respectively. A reactive plasma was generated by RF powers of 30 - 150 W with 95% argon (Ar) and 5% H_2O mixed gas. By an electrostatic probe measurement, plasma temperature and density were obtained to be 11 - 14 eV and $4 - 5 \times 10^{16}$ m^{-3}, respectively, for a gas flow rate of 20 sccm and total pressure of 100 Pa. The temperature (the density) increased with increasing RF power; meanwhile, they were almost independent of radial distances with ranges of 6 - 16 mm.

As shown in Fig. 1, H_2O gas was produced from an H_2 gas flowing through an oxidation-reduction reactor. The reactor was filled with copper oxide (CuO) pebbles with diameters of 0.7 - 1.2 mm and was heated up to 350°C, where the oxidation-reduction reaction proceeded as $CuO + H_2 \rightarrow Cu + H_2O$. Figure 2 shows typical time variations of partial pressures of H_2 and H_2O measured at the end of the plasma reactor using a quadrupole mass spectrometer (QMS/ULVAC BGM-102). With heating the CuO pebbles in an electric furnace, the H_2 gas was gradually replaced by H_2O gas, as shown in Fig. 2. More than 98% of H_2 gas was converted into H_2O gas when reaching the maximum temperature of 350°C. The CuO pebbles can be regenerated by replacing H_2 gas with oxygen gas (O_2) in the reactor.

To investigate the effect of C deposition, a vessel wall of the plasma reactor was covered with C depositions via decomposition of CH_4 gas. A mixed plasma was generated by introducing a 90% Ar and 10% CH_4 with a total pressure of 100 Pa, flow rate of 20 sccm, and RF power of 60 W. To observe the composition changes near

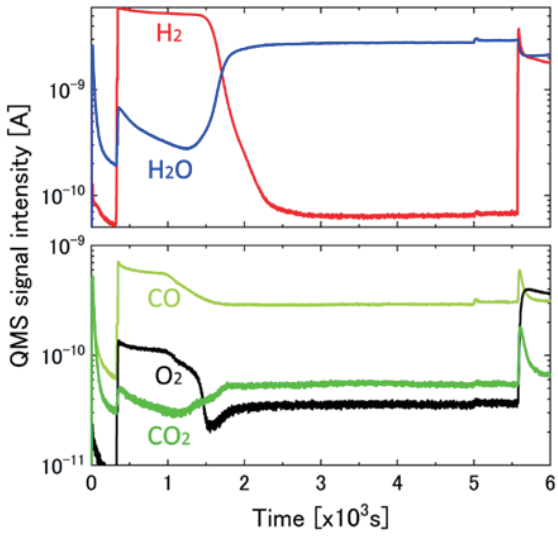

Fig. 2 Time variations of deoxidation of cupper-oxide pebbles heated in an H_2 gas. The signal intensities for H_2 , H_2O, CO, O_2, and CO_2 were measured at the end of a plasma reactor.

the wall surface, three specimens (made of stainless steel, 150 mm × 5 mm × 0.1 mm) were set on the vessel wall, as shown in Fig. 1. The surface composition of the specimens was analyzed through an energy-dispersive X-ray spectrometer (EDS/JSM-IT500). Table 1 presents the EDS results for specimen 2 before and after C deposition. The original surface consists of several elements, such as iron (Fe), C, chromium (Cr), and nickel (Ni), generally observed in stainless steel. After 2 hours of exposure to the

Table 1 Surface composition by EDS analysis.

Elements	Concentrations (%)		
	Before deposition	After deposition	operation by 3 hours
Fe	53		66
C	18	100	2
Cr	15		17
Ni	10		9
Others	4	0	6

Ar-CH_4 mixed plasma, only C was detected on the specimen surface. This indicated that the surface was perfectly covered by the deposition of C dust produced by CH_4 decomposition in the plasma.

During experiments on H_2O decomposition in the plasma, the partial pressures of gases with mass-to-charge ratio (m/z) of 2 (H_2), 18 (H_2O), 28 (CO), 32 (O_2), and 44 (CO_2) flowing out from the plasma reactor were observed using QMS. Here we define the decomposition ratio as the molecular ratio in the percentage of H_2O decomposed in the plasma. The decomposition ratio of H_2O (m/z = 18) was derived from the ratio, $R_{on/off}$, of QMS signal intensities when the plasma was turned on to off. Therefore, the decomposition rate was estimated to be 1-$R_{on/off}$.

2.2 Calibration method relating QMS signal to the partial pressure of different gas species

Real partial pressures for mass species i, P_i, can be evaluated from the observed intensities of QMS signals using the following relation according to [13]:

$$P_i = P_{H_2O}\frac{(I_i/I_{H_2O})}{(E_i/E_{H_2O})(T_i/T_{H_2O})(D_i/D_{H_2O})} = P_{H_2O}\frac{I_i}{I_{H_2O}}C_{i,H_2O} = \alpha_{H_2O}I_iC_{i,H_2O}, \quad (1)$$

where I_i and I_{H_2O} are the signal intensities of species i and H_2O, respectively; P_{H_2O} is the partial pressure of H_2O. The E_i (E_{H_2O}), T_i (T_{H_2O}), and D_i (D_{H_2O}) are the efficiencies of ionization for gas species i (H_2O), those of transmission of the ionized species in a quadrupole filter, and those of detection in an ion detector, including gain of electron multiplier, respectively, in QMS. Since the efficiencies generally depend on the mass of species, the observed intensities I_i for different masses must be calibrated to evaluate partial pressures with standard leaks for relevant gas species. Instead of each calibration process, a simple method was used in this study with mass-dependences of the ratios of the efficiencies for each species to those for H_2O. The ratio E_i/E_{H_2O} was estimated from partial cross-sections for each species to lose an electron by the impact of an electron with tens of eV [14, 15]. Table 2 presents the estimated ratios for electron energy of 50 eV resulting from an ionization voltage chosen in our experiment.

The ions with high masses were weakly focused to be lost on quadrupole rods in the filter. This causes the transmission efficiency T_i to depend on the distribution of potential made by the rods, which should be inversely proportional to the mass of relevant species [16]. However, the efficiency is well known to be influenced by the design, construction, and contamination of the rods [17]. Therefore, a correction was included in the detection efficiency D_i according to ref. [13]. Since the corrected efficiency D_i was approximately proportional to the square root of mass, a mass-dependent factor, C_{i,H_2O}, defined as $1/(E_i/E_{H_2O})(T_i/T_{H_2O})(D_i/D_{H_2O})$, is evaluated as in Table 2. In parentheses, the ratios were also presented for efficiencies D_i depending on the mass to the power of 0.54. The value of which was estimated from experimental ones in ref. [13] using the least square approximation. Thus, the partial pressure of each species is proportional to I_i multiplied by C_{i,H_2O}, as shown in eq. (1), where α_{H_2O} is a calibration factor in PaA^{-1}, relating QMS signal for H_2O to the partial pressure of H_2O. Assuming 5 Pa (5% of 100 Pa) and QMS signal intensity of 2.77×10^{-9} before plasma ignition, each partial pressure of reaction products can be estimated using α_{H_2O} = 5 Pa/(2.77×10^{-9} A) = 1.80×10^{9} PaA^{-1}.

Table 2 Mass-dependent factors, C_{i,H_2O}, relating partial pressure of each gas species, i, to QMS signal. E_i/E_{H_2O} is the ratio of ionization efficiencies for each species, i, to H_2O.

Gas species, i	m/z	E_i/E_{H2O}	$C_{i,H2O}$
H_2	2	0.83	0.40 (0.44)
H_2O	18	1	1
CO	28	1.48	0.84 (0.83)
O_2	32	1.04	1.28 (1.25)
CO_2	44	1.64	0.95 (0.92)

*The C_{i,H_2O} values in parentheses correspond to those estimated from experimental mass-dependence of D_i [13] in eq. (1) using the least square approximation.

3. Results

3.1 Decomposition of water vapor in a plasma reactor

Figure 3 shows an example of H_2O decomposition experiments before C deposition (the vessel wall was an original surface of stainless steel). An Ar-H_2O mixed plasma was turned on 6 times for 10 min each at intervals of 5 min. The RF power was changed to 30, 60, 90, 120, and 150 W for each. The total pressure of the mixed gas and the flow rate were 100 Pa and 20 sccm, respectively.

By each plasma ignition, the partial pressure of H_2O was decreased, whereas the pressures of H_2 and O_2 were significantly increased. The increases in H_2 and O_2 signals must be attributed to the decomposition of H_2O by the plasma. The increase in the pressures of H_2 at lower RF

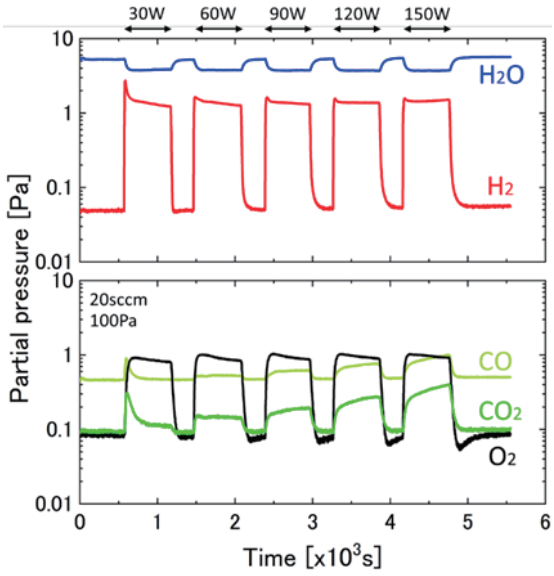

Fig. 3 Time variations of partial pressures of H_2, H_2O, CO, O_2 and CO_2 in a plasma reactor. The vessel wall was made of a stainless steel.

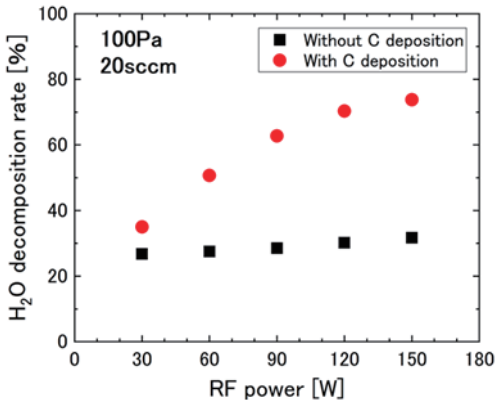

Fig. 4 Dependence of decomposition ratio on the RF power, with and without C deposits on the vessel wall.

powers was accompanied by a pulse-like increase immediately after turning on the plasma. Also, the pulse-like increase was found for CO and CO_2. These pulse-like increases might result from the reemission of absorbed gases on the wall. The decrease in the pressures of H_2O was not largely dependent on the RF power. However, the pressures of CO and CO_2 continued to increase during turning on the plasma and were increased with increasing RF power. The C component of the gases originates from the surface of a vessel wall. Since C and O atoms react easily due to their large binding energy [18], some O atoms were incorporated into the molecules at an elevated temperature of the vessel wall; the temperature was about 40°C at the RF power of 30 W, whereas it increased to about 110°C at 150 W.

The decomposition ratio was evaluated to be 1- $R_{on/off}$ from the ratio $R_{on/off}$ (a ratio of a QMS signal during the plasma to one without plasma). Figure 4 shows the result (closed squares) as a function of the RF power. The decomposition ratio was around 30% and demonstrated approximately no dependence (or slightly increased) on RF power from 30 to 150 W. The decomposition ratio (about 30%) with stainless steel walls was about half of that with a vycor wall reported by Roychowdhury *et al.* [7]. They determined the decomposition ratio by weighing H_2O flowing out of the reactor and then condensing in a cold trap after a 30-min discharge. Our power density ranged from 0.13 to 0.63 Wcm^{-3}, which was comparable to their densities (about 0.1 to 0.5 Wcm^{-3}). The decomposition ratio decreased due to the short residence time of H_2O molecules in the plasma zone, resulting in fewer collision events with plasma electrons. The residence time was calculated from the flow rate and operating pressure in the plasma (the volumes of plasma were about 240 cm^3 in our device and 100 cm^3 in their device). Our gas flow rate and pressure were 20 sccm (1 sccm for H_2O) and 100 Pa (5 Pa for H_2O), respectively, whereas theirs were 0.27 - 1.0 sccm (0.72 - 2.68 mmol hr^{-1}) and ~43 Pa (0.32 Torr), respectively. The calculation results showed that our residence time was 0.64 s, much shorter than theirs (2.3 - 8.6 s). This may explain the low decomposition ratios in our cases. Additionally, a high RF power experiment from 250 to 1,000 W was recently performed with a quartz tube by Nguyen *et al.* [8]. They showed decomposition ratios of 44% and 36% at flow rates of an H_2O-Ar mixed gas, 35 and 85 sccm, respectively, at the pressure of ~40 Pa (0.3 Torr). However, their power density was relatively small to be 0.03 to 0.11 Wcm^{-3} due to their large plasma volume (~8,800 cm^3). The residence time was calculated from the gas flow rates to be 5.5 and 2.3 s, respectively. Also, this may explain the reason for slightly higher decomposition ratios than ours, although the power density was lower.

3.2 Effect of C deposition on decomposition ratio in a plasma reactor

Figure 5 shows the result of the H_2O decomposition experiment with C deposition on the vessel wall. The gas pressure and the gas flow rate in the reactor were the same as in Fig. 3. The RF power was changed in the order of the strength, being opposite to the case in Fig. 3. The pulse-like increase in Fig. 3 vanished in the pressures of H_2, CO, and CO_2 since the gases adsorbed on the vessel wall could be suppressed due to C deposition on it [19]. The H_2O pressure decreased more than that of Fig. 3. The pressures of H_2 and CO were more than the pressures of no C deposition case (Fig. 3), and the CO_2 pressure was increased in particular at low RF power. However, the O_2 pressure was drastically changed. For no C deposition case (Fig. 3), the pressure was increased with plasma ignition. In contrast, it was decreased by C deposition on the wall, except for the case of the lowest RF power (30 W). Furthermore, the

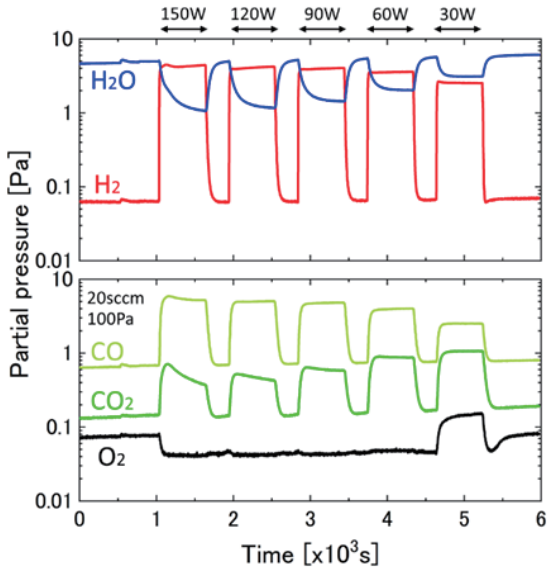

Fig. 5 Time variations of partial pressures of H_2 , H_2O, CO, O_2 and CO_2 in a plasma reactor. The vessel wall was covered by C deposits.

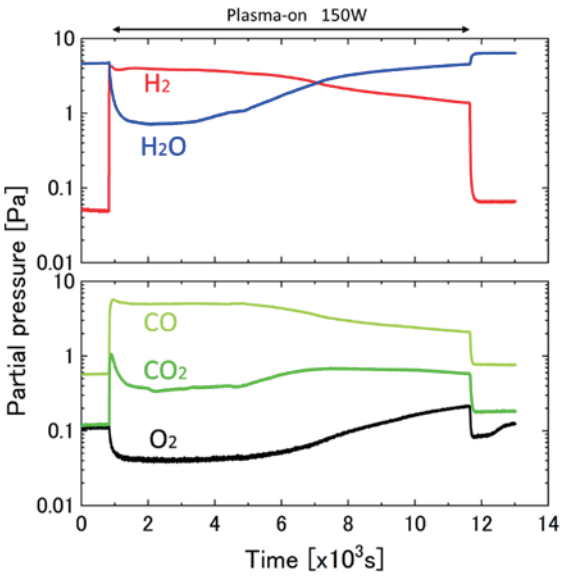

Fig. 6 Temporal variation of partial pressures of H_2, H_2O, CO, O_2 , and CO_2 in a long-term (3 h) and high-power (150 W) operation.

O_2 pressure after turning off each plasma was kept to be the same level as the case when the plasma was turned on. These findings indicate that O products by decomposition of H_2O were converted to CO and CO_2 through the interaction with C depositions on the vessel, such as chemical sputtering of C depositions by the impact of low-energy O atoms or ions.

The closed circles in Fig. 4 show the decomposition ratio with C deposition. The decomposition ratio was higher for the C deposition case and largely increased from 35% to 75% with the RF power. Since the increase in the RF power resulted in a higher temperature of plasma electrons (e.g., ~ 11 and ~ 14 eV at 30 and 150 W, respectively), a higher decomposition ratio can be expected in the case of high RF power. The conversion of O products to carbon oxides may cause the ratio to be high at high RF power due to a suppression of the inverse reaction (recombination of O and H products to reproduce H_2O). Further discussion on the mechanism is presented in the next section.

3.3 Long-term operation of plasma reactor with carbon deposition

A long-term operation of the plasma reactor with C deposition was examined to continuously decompose H_2O. Figure 6 shows the result of continuous operation with an RF power of 150 W for 3 h. In an early stage of operation (<about 1 h), the H_2O decomposition ratio was kept high. However, after ~ 4,000 s, the decomposition ratio gradually decreases (H_2O pressure gradually increases), accompanied by the increase in the O_2 pressure. When the plasma was turned off, a stepwise increase in the pressure for H_2O and decrease in the pressures for H_2, O_2, CO, and CO_2 were observed. The increase and decrease amounts of the pressures, except for O_2, were close to the amounts for the original wall (no deposition) case, as found in Fig. 3. This causes us to expect the removal of C depositions on the wall due to the long-time operation. Table 1 presents the result of elemental analysis after this long-term operation. The C depositions perfectly disappeared, and several elements included in the original material were observed. Furthermore, the C component in the material was reduced due to an interaction with plasma ions, probably chemical sputtering by O atoms or ions.

4. Discussion

In this section, decomposition mechanisms inherent in this experiment were discussed using the reaction rate equation in equilibrium and mass balance of H_2O injected to decomposition products.

4.1 Discussion of reaction rate equation

When the reaction rate per unit time and unit volume, R, is proportional to the concentration, C, of H_2O in a plasma reactor [20], the rate constant k_r in a unit of s^{-1} is estimated from the rate equation,

$$\ln \frac{C_{\text{out}}}{C_{\text{in}}} = -k_r \frac{V}{Q}, \tag{2}$$

where C_{in} and C_{out} are H_2O concentrations in inlet and outlet, respectively; V is the reaction volume in m^3; Q is the gas flow rate in m^3s^{-1}. If the inverse reaction, i.e., recombination of decomposition products by themselves, occurs negligibly small, the rate constant is related to the rate coefficient $\langle \sigma v \rangle$ for dissociative collisions experienced by in-

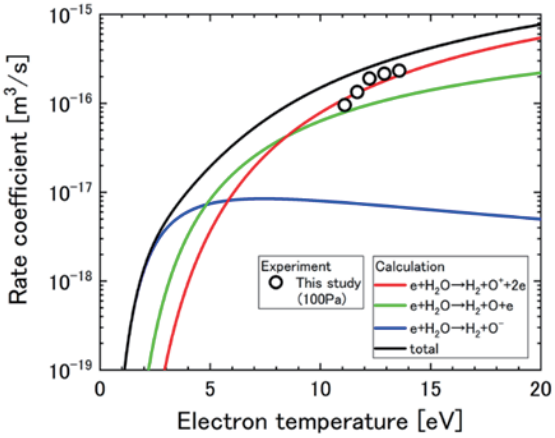

Fig. 7 Comparison of rate coefficients obtained experimentally with those calculated by using collision cross sections for relevant dissociations of H_2O.

jected H_2O molecules with plasma electrons as follows:

$$\langle \sigma v \rangle = \frac{R}{n_e n_{H_2O}} = \frac{k_r n_{H_2O}}{n_e n_{H_2O}} = \frac{k_r}{n_e}, \quad (3)$$

with the volume densities in m^{-3}, n_e, and n_{H_2O}, of plasma electrons and neutral H_2O molecules, respectively. To eliminate the effect of inverse reactions as possible, the rate constant in eq. (2) was estimated using the ratio C_{out}/C_{in} observed experimentally in the case of C deposition (Fig. 5), where O products were almost converted into CO and CO_2. Figure 7 shows the rate coefficients obtained by substituting the estimated k_r into eq. (3) plotted as a function of plasma electron temperature, corresponding to various RF powers. Here, the temperature measured by a thermocouple attached to the outer surface of the vessel wall (Fig. 1) was tentatively used as the gas temperature of H_2O to convert the flow rate in sccm to that in volume $[m^3 s^{-1}]$.

Also, the rate coefficient $\langle \sigma v \rangle$ can be evaluated by integrating the relevant collision cross-section $\sigma(E)$ with the electron energy E over a Maxwellian distribution as follows:

$$\langle \sigma v \rangle = \left(\frac{8 k_B T_e}{\pi m} \right)^{1/2} \int_{E_{th}}^{\infty} \sigma(E) \left(\frac{E}{k_B T_e} \right) \times \exp\left(-\frac{E}{k_B T_e} \right) d\left(\frac{E}{k_B T_e} \right), \quad (4)$$

where T_e and m are the temperature and mass of plasma electrons, respectively; E_{th} is the threshold energy for the relevant collisions; k_B is the Boltzmann constant. To estimate $\langle \sigma v \rangle$ from eq. (4), three reactions,

$$e^- + H_2O \rightarrow H_2 + O + e^-, \quad (5)$$

$$e^- + H_2O \rightarrow H_2 + O^+ + 2e^-, \quad (6)$$

$$e^- + H_2O \rightarrow H_2 + O^-, \quad (7)$$

were considered as relevant dissociative collisions with electrons. The partial cross-sections were taken from ref. [21]. Also, Fig. 7 shows the calculated rate coefficients as a function of the plasma electron temperature up to 20 eV. The rate coefficients increased with increasing temperature, except for the O^- production to be a small component of our plasma temperatures. The rate coefficients obtained experimentally (open circles) were reasonably consistent with the calculated coefficients. This agreement might indicate that the enhancement of decomposition ratio for H_2O molecules with C deposition on a vessel wall was caused by the removal of O products from the plasma, resulting in suppression of inverse reactions (recombination of H and O products) to reproduce H_2O. However, the sum of rate coefficients for O, O^+, and O^- products was larger than the experimental ones, probably due to some inverse reactions.

Another possible reason for the enhancement of the decomposition ratio observed with C deposition may be the so-called water-gas shift (WGS) reaction with CO,

$$CO + H_2O \rightarrow CO_2 + H_2. \quad (8)$$

In the reaction, CO can be converted into CO_2, and H_2O is decomposed, as recently investigated using a surface-wave microwave discharge by Chen *et al.* [22]. Further discussion on the contribution to our mechanism is presented in the next subsection.

4.2 Discussion on mass balance

In this subsection, the mass balance of injected H_2O with observed products, H_2, O_2, CO, and CO_2, in a plasma reactor is discussed. The molecular ratio for each of the gas species, i, to injected H_2O was estimated using mass-dependent factors, $C_{i,H2O}$ to be P_i/P_{H_2O}. According to eq. (1), P_i/P_{H_2O} was calculated from the ratio of the increment of each QMS signal to the decrement of the H_2O signal, I_i/I_{H_2O}. Table 3 presents the P_i/P_{H_2O} values for experiments with and without C deposition at RF powers of 30 to 150 W. For different RF powers, the ratios of the increments in QMS signal intensities for H_2, O_2, CO, and CO_2 to the decrement in the intensity for H_2O at a moment of 25 s before turning off the plasma were taken as I_i/I_{H_2O} because the intensities were considered to be approximately in equilibrium.

The ratio of partial pressure of O_2 to that of H_2O was close to 0.5 in the case of no C deposition, indicating that the O_2 molecules originated from the decomposition of H_2O injected into the plasma reactor. However, the partial pressure of H_2 was smaller than the unity expected from the decomposition. In addition to the ambiguity of strong mass dependence of D_i, another possible reason may be inevitable ambiguities for the ionization efficiencies (i.e., ionization cross-sections) used for the calculation, e.g., 10% or more for H_2 at energies of tens of eV [14]. The partial pressures of CO and CO_2 were small at low RF power (30 W), whereas increased power gradually increased the pressures.

Large differences were found in the composition of

Table 3 Ratios P_i/P_{H_2O} of partial pressures of H_2 , CO, O_2, and CO_2 to the pressure of H_2O, calculated using mass-dependent factors C_{i,H_2O}. The values in parentheses correspond to those with C_{i,H_2O} estimated from the experimental dependence of D_i on the mass of gas species [13] using the least square approximation.

Gas species, i (m/z)	RF power (W)									
	30	60	90	120	150	30	60	90	120	150
	Before C deposition (stainless steel)					After C deposition				
	P_i/P_{H2O}					P_i/P_{H2O}				
H_2 (2)	0.83 (0.90)	0.84 (0.92)	0.84 (0.91)	0.81 (0.89)	0.86 (0.93)	0.97 (1.06)	1.05 (1.15)	1.08 (1.18)	1.11 (1.21)	1.12 (1.22)
H_2O (18)	1	1	1	1	1	1	1	1	1	1
CO (28)	0.00 (0.00)	0.04 (0.04)	0.10 (0.10)	0.18 (0.17)	0.30 (0.29)	0.68 (0.67)	0.98 (0.96)	1.11 (1.09)	1.16 (1.14)	1.17 (1.15)
O_2 (32)	0.51 (0.49)	0.52 (0.51)	0.53 (0.52)	0.51 (0.50)	0.49 (0.48)	0.04 (0.04)	0.00 (0.00)	0.00 (0.00)	0.00 (0.00)	-0.01 (-0.01)
CO_2 (44)	0.01 (0.01)	0.03 (0.03)	0.06 (0.06)	0.11 (0.11)	0.18 (0.17)	0.35 (0.34)	0.21 (0.21)	0.12 (0.11)	0.08 (0.08)	0.06 (0.06)

gases observed with C deposition on the vessel wall. Except for the 30 W case, O_2 molecules that originated from the decomposition of injected H_2O molecules were absent and replaced mostly by CO molecules. Furthermore, the partial pressure of H_2 was higher than that for the no deposition case. Since C depositions were produced by adding 10% CH_4 gas to an Ar gas in the plasma reactor, they contained many H atoms, probably by forming the so-called amorphous hydrogenated carbon (a-C:H) [23]. Therefore, H atoms in the depositions might be emitted in the form of hydrocarbons by impacts of plasma ions. The partial pressures for $m/z = 16$ (CH_4) and 30 (C_2H_6) at an RF power of 150 W were 0.016 (0.08 Pa) and 0.022 (0.11 Pa), respectively, which were much lower than that of H_2O. However, the hydrocarbon demonstrated nonnegligible contributions to H_2 production via their dissociation because the partial pressures of H_2 produced by the dissociation were estimated to be 0.032 ($= 0.016 \times 2$) and 0.066 ($= 0.022 \times 3$) in maximum. Therefore, the chemical sputtering of C depositions by the impact of H products (atoms, molecules, and those ionized) may lead to the additional production of H_2 molecules.

The C-based materials are well known to be eroded chemically by low-energy O ions by emitting carbon oxides, mainly CO (also CO_2). The yield has been more than 0.5 at the tens of eV energy range [24]. The yield is larger than the chemical sputtering yield (< 0.1) by impacts of H ions (forming hydrocarbons) [25], probably due to the higher binding energy of C with O than with H [18]. Because the partial pressures of hydrocarbons, such as CH_4 ($m/z = 16$) and C_2H_6 ($m/z = 30$), were low (~ 0.02 relative to H_2O), the partial pressure of $m/z = 28$ was thought to be dominated by CO instead of C_2H_4. The neutral O products are ionized due to frequent collisions with plasma electrons and accelerated with O^+ products by a plasma sheath (roughly $3T_e$ [24] to be ~40 eV in our case) before impacts on the wall. Therefore, CO (also CO_2) molecules observed in our experiment might be originated from chemical erosion of C depositions due to impacts of the neutral and ionized O products.

The WGS reaction in eq. (8) may be another possible reason for enhancing H_2O decomposition. With decreasing RF power, the pressure of CO decreased, and that of CO_2 increased, whereas their sum remained roughly unchanged (~ 1.2 except for 30 W). Because H_2 was produced via the WGS reaction, the pressure of H_2 remains higher than in the no C deposition case. The highest RF power (150 W) caused the decomposition ratio to be maximum (75%), where the partial pressure of CO_2 was much lower than that of CO. This discrepancy indicated a small contribution to the reaction, at least at high RF powers.

5. Conclusions

A flow-type plasma reactor using an RF power was applied to decompose H_2O, exhausted from the plasma vessel in a fusion reactor. An H_2O gas produced by deoxidation of CuO pebbles heated in H_2 gas was mixed with Ar gas at a concentration of 5% and introduced into the plasma reactor. The effect of C deposition on the vessel wall was investigated to explore the possibility of improving the decomposition ratio. Then, a stainless steel wall was covered by C before the experiment by introducing an Ar gas containing CH_4 of 10% in the reactor. The decomposition ratio of H_2O was evaluated from the ratio of the QMS signals for H_2O when the plasma was turned on to off. To obtain the ratio of the pressures to that of the injected H_2O, the mass-dependent factors relating partial pressures of decomposition products to their QMS signals were evaluated.

For an original vessel wall (no C deposition case), the pressure of H_2O was decreased by turning on the plasma, and the pressures of H_2 and O_2 were increased to be those for the decomposition products. The decomposition ratio was around 30% at the gas flow rate of 20 sccm (1 sccm for H_2O) and the total gas pressure of 100 Pa (5 Pa for H_2O), and the ratio was slightly increased with increasing RF power of 30 to 150 W. For the C deposition case, the decomposition ratio was significantly increased from 35% to 75% with increasing RF power under the same conditions. The large increase in the ratio was accompanied by a substantial increase and decrease in the pressures of CO and O_2, respectively. This indicated that O products by decomposition of H_2O reacted to produce CO molecules through the interaction with C depositions. The reduction

of O products may suppress any inverse reaction (recombination of H and O products) to reproduce H_2O in the plasma. Furthermore, a WGS reaction may improve the decomposition ratio. After the long-term operation of 3 h of the reactor, the decomposition ratio was decreased to be the ratio of the original wall, and C depositions certainly disappeared.

In a previous experiment on CH_4 decomposition [9], hydrocarbon films (e.g., a-C:H) deposited on a vessel wall reduced H recovery efficiency. Since the C depositions are eroded by the decomposition of H_2O, as discussed in this study, subsequent or simultaneous decompositions of hydrocarbons and H_2O can be expected to recover hydrogen isotopes efficiently. The flow-type plasma reactor allows us to simplify the recovery process in the fuel cycle system for a fusion reactor (e.g., TEP in ITER) because chemical reactors require different systems for each chemical compound. To demonstrate the efficient simultaneous decomposition of H_2O and hydrocarbons, further detailed experiments will be necessary.

Acknowledgment

This work was supported by the Grant-in-Aid for Scientific Research of JSPS KAKENHI (21K13899). The author (M.O.) would like to acknowledge Dr. K. Ohya for his useful discussion.

[1] T. Tanabe, J. Nucl. Mater. **438**, S19 (2013).
[2] T. Yamanishi, *Tritium: Fuel of Fusion Reactors*, edited by T. Tanabe (Springer Japan, 2017) chap. 6.
[3] J. Wilson *et al.*, Fusion Sci. Technol. **75**, 794 (2019).
[4] M. Glugla *et al.*, Fusion Eng. Des. **82**, 472 (2007).
[5] K. Isobe *et al.*, Fusion Sci. Technol. **41**, 988 (2002).
[6] A. Fridman *Plasma Chemistry* (Cambridge Univ. Press, 2008) p.1.
[7] S. Roychowdhury *et al.*, Plasma Chem. Plasma Proc. **2**, 157 (1982).
[8] S.V.T. Nguyen *et al.*, Rev. Sci. Instrum. **80**, 083503 (2009).
[9] K. Katayama *et al.*, Fusion Eng. Des. **85**, 1381 (2010).
[10] K. Katayama *et al.*, Fusion Sci. Technol. **60**, 1379 (2011).
[11] K. Katayama *et al.*, Fusion Sci. Technol. **71**, 426 (2017).
[12] M. Oya *et al.*, Plasma Fusion Res. **15**, 2405032 (2020).
[13] N. Hirashita *et al.*, J. Vac. Soc. Jpn. **57**, 214 (2014) [in Japanese].
[14] R.K. Janev *et al.*, *Elementary Processes in Hydrogen-Helium Plasmas* (Springer, Berlin, 1987) p.52 and p.241.
[15] J.W. McConkey *et al.*, Phys. Reports **466**, 1 (2008).
[16] E. Hoffman and V. Stroobant, *Mass Spectrometry* (John Wiley & Sons, The Atrium, 2007) p.96.
[17] *Quadrupole Mass Spectrometry and its Applications*, edited by P.H. Dawson (Elsevier, Amsterdam, 1976) p.121.
[18] *Handbook of Chemistry and Physics*, 95th edited by. W.M. Haynes (CRC Press, Boca Raton, 2014) p.9-65.
[19] J. Winter, J. Nucl. Mater. **145-147**, 131 (1987).
[20] P. Atkins *et al.*, *Physical Chemistry*, 11th ed. (Oxford Univ. Press, Oxford, 2018) p.725.
[21] Mi-Y. Song *et al.*, J. Phys. Chem. Ref. Data **50**, 023103 (2021).
[22] G. Chen *et al.*, Int. J. Hydrogen Energy **40**, 3789 (2015).
[23] R.E. Clausing and L. Heatherly, J. Nucl. Mater. **145-147**, 317 (1987).
[24] *Physical Processes of the Interaction of Fusion Plasma with Solids*, edited by W.O. Hofer and J. Roth (Academic Press, San Diego, 1996) p.112 and p.156.
[25] *Sputtering by Particle Bombardment*, edited by R. Behrisch and W. Eckstein (Springer, Berlin, 2007) p.329.